



Published in final edited form as:

Gene Ther. 2004 December ; 11(23): 1675–1684.

Safety and biodistribution studies of an HSV multigene vector following intracranial delivery to non-human primates

D Wolfe¹, A Niranjan², A Trichel¹, C Wiley³, A Ozuer¹, E Kanal², D Kondziolka², D Krisky³, J Goss⁴, N DeLuca¹, M Murphey-Corb¹, and JC Glorioso¹

¹ Department of Molecular Genetics and Biochemistry, University of Pittsburgh School of Medicine, Pittsburgh, PA, USA

² Department of Neurosurgery, University of Pittsburgh School of Medicine, Pittsburgh, PA, USA

³ Department of Pathology, University of Pittsburgh School of Medicine, Pittsburgh, PA, USA

⁴ Department of Neurology, University of Pittsburgh School of Medicine, Pittsburgh, PA, USA

Abstract

Malignant glioma is a fatal human cancer in which surgery, chemo- and radiation therapies are ineffective. Therapeutic gene transfer used in combination with current treatment methods may augment their effectiveness with improved clinical outcome. We have shown that NUREL-C2, a replication-defective multigene HSV-based vector, is effective in treating animal models of glioma. Here, we report safety and biodistribution studies of NUREL-C2 using rhesus macaques as a model host. Increasing total doses (1×10^7 to 1×10^9 plaque forming units (PFU)) of NUREL-C2 were delivered into the cortex with concomitant delivery of ganciclovir (GCV). The animals were evaluated for changes in behavior, alterations in blood cell counts and chemistry. The results showed that animal behavior was generally unchanged, although the chronic intermediate dose animal became slightly ataxic on day 12 postinjection, a condition resolved by treatment with aspirin. The blood chemistries were unremarkable for all doses. At 4 days following vector injections, magnetic resonance imaging showed inflammatory changes at sites of vector injections concomitant with HSV-TK and TNF α expression. The inflammatory response was reduced at 14 days, resolving by 1 month postinjection, a time point when transgene expression also became undetectable. Immunohistochemical staining following animal killing showed the presence of a diffuse low-grade gliosis with infiltrating macrophages localized to the injection site, which also resolved by 1 month postinoculation. Viral antigens were not detected and injected animals did not develop HSV-neutralizing antibodies. Biodistribution studies revealed that vector genomes remained at the site of injection and were not detected in other tissues including contralateral brain. We concluded that intracranial delivery of 1×10^9 PFU NUREL-C2, the highest anticipated patient dose, was well tolerated and should be suitable for safety testing in humans.

Keywords

cancer; primate; TNF α ; glioma; HSV

Introduction

Treatment of glioblastoma multiforme by surgical resection and chemo- and radiation therapy are only palliative resulting in a poor patient prognosis.¹⁻³ Molecular medicines including

gene transfer-based therapies used in combination with one or more standard approaches may provide a more powerful treatment strategy and could involve synergy among the therapeutic modalities. The base vector used for our studies is a replication-defective HSV type 1 vector deleted for multiple essential immediate-early (IE) genes and derived from a previously described mutant virus.^{4,5} This vector was modified to contain an IE form of the thymidine kinase gene and also expressed the IE gene encoding infected cell protein zero (ICP0).⁶ ICP0 was previously shown to enhance transgene expression and arrest cell cycle progression, a phenomenon also expected for rapidly dividing tumor cells.^{5,6} ICP0 is rapidly degraded in neuronal cells, suggesting that infection of normal brain should not result in ICP0-related toxicity.⁴ This vector platform therefore may be ideal for high-level transient antitumor gene expression while inhibiting tumor cell growth.

Suicide gene therapy by delivery of HSV-TK in combination with ganciclovir GCV provides a direct toxic effect to dividing tumor cells. Gap junctions mediate transfer of HSV-TK-activated GCV to nontransduced tumor cells, resulting in bystander cell killing by apoptosis. Several vector systems have been used to deliver HSV-TK in combination with GCV, but human clinical trials have failed to provide effective treatment using tk-activated GCV as the sole therapy.⁷⁻⁹ The bystander effect is improved by coexpression of connexin 43 (Cx43) and HSV-TK,¹⁰⁻¹² and we have confirmed these findings using our platform vector further engineered to express Cx43 in animal models of glioblastoma *in vivo*.^{13,14}

Gamma-knife radiosurgery (GKR) allows precise delivery of a single high dose of radiation to brain tumors without opening the skull. Tumors are targeted by the application of a tightly focused high-energy radiation field with minimal collateral damage to the surrounding normal tissue.^{15,16} Unfortunately, glioma tumor cells often invade normal brain tissue surrounding the tumor and migrate along normal white matter tracts. This feature of glioma is largely responsible for the ineffectiveness of surgical tumor resection. The synergistic effect of radiation and TNF α on a variety of tumors provides an additional combinatorial approach to increasing the effectiveness of experimental therapies.¹⁷⁻¹⁹ Chung *et al.*²⁰ Rasmussen *et al.*²¹ and Staba *et al.*²² found inducible TNF expression (TNFerade) combined with radiation was superior to either treatment alone. Similarly, the response to GKR was enhanced by sensitizing experimental tumors with vector-expressed TNF α using our HSV vector system in combination with GKR.²³

To further take advantage of multigene treatments, we engineered a multigene vector (NUREL-C2) that simultaneously expressed all four transgenes (HSV-TK, ICP0, Cx43, and TNF α) and applied this vector in a multimodal experimental glioma treatment regimen involving the vector, GCV and GKR.¹⁴ This multimodal treatment strategy proved superior to both individual and paired treatments, providing support for this combination treatment strategy to human glioma. As part of the toxicological evaluation required for early Phase I safety testing in humans with malignant glioma, we examined the expression, histopathology, and biodistribution of intracranially delivered NUREL-C2 in combination with GCV in normal brain of rhesus monkeys (*Macaca mulatta*).

Results

Vector stocks

Previous studies have demonstrated that all four transgenes are expressed by our multigene vector and that the structure of NUREL-C2 (Figure 1) was stable with passage.¹⁴ Prior to use in preliminary safety studies in animals, virus stocks were tested for the presence of replication-competent virus recombinants (RCV) that could potentially arise from rescue of ICP4 and ICP27 during virus vector production in complementing cells. The presence of RCV could cause toxicity and alter vector distribution in animals. To minimize RCV generation, the E11

complementing cell line was engineered to contain minimal homology between the essential genes ICP4 and ICP27 absent in the vector and present in the cell line.²⁴ Since two essential virus genes must be rescued in order to restore virus replication, the frequency of double gene rescue is predictably extremely small and conservatively estimated at $>10^{-14}$ based on evidence that rescue of a single gene (eg ICP4) was not detected in $>10^{-8}$ plaque forming units (PFU).²⁵

The sensitivity of our replication-competent detection assay was validated by the ability to detect viral replication when 3 PFU of wild-type virus (KOS) was added to 1×10^8 or 1×10^9 PFU aliquots of NUREL-C2 (Table 1). The use of 3 PFU wild-type virus provides a 99.5% level of confidence by Poisson's distribution such that at least one PFU was added to the vector test stock. The results showed that no RCV was detected in the vector stocks used for the highest vector doses (10^8 and 10^9). Moreover, the presence of high levels of vector did not interfere with wild-type virus replication since the NUREL-C2 samples with added wild-type virus showed cytopathic effect (CPE) in all cases. These findings ensured that vector stocks used in these primate safety studies were unlikely to contain RCV.

Primate studies

We delivered increasing doses of NUREL-C2 into rhesus brain via a craniotomy. The total vector dose contained in 0.1 ml was distributed in ten 0.01 ml aliquots and delivered in a circular manner, simulating injection into the borders of an intracranial tumor. GCV was delivered to the bloodstream in a continuous manner using a surgically implanted osmotic pump in order to sustain GCV levels. A general flowchart of the procedures is presented in Figure 2, and the specific animal information and physical data is presented in Table 2. All animals were monitored twice daily and given a physical examination prior to sample collection, surgery, or imaging. With the exception of macaque M0901, all animals remained clinically normal following intracerebral inoculation with NUREL-C2. All animals displayed normal locomotion, activity, appetite, hydration, and both stool and urine output. Macaque M0901 was clinically normal following NUREL-C2 inoculation, but became slightly ataxic 7 days following a magnetic resonance imaging (MRI)/cerebrospinal fluid (CSF) collection procedure (day 12 postinoculation). This animal received an intermediate (1×10^8 PFU) vector dose, and it is unclear whether the vector or the MRI/CSF procedures were responsible for this transient behavior. This animal responded to nonsteroidal inflammatory treatment (11 mg/kg twice daily for 3 days) and returned to a clinically normal state and remained clinically normal until killing at day 35 postinoculation.

Blood cell and chemistry analysis

Systemic toxicity of an experimental therapy can be evaluated initially using standard blood cell and blood chemistry analysis. Four of the five macaques exhibited a mild monocytosis (range 8–11%; reference range 1–4%) on day 4 following intracranial injection of the NUREL-C2 vector; however, monocytosis was also present at the start of the experiment and may be related to animal handling rather than vector inoculation. Two of these four monkeys were killed after 4 days, while the remaining two animals were killed after 4 weeks. Of the long-term animals, one had a mild but persistent monocytosis, while the other did not show a monocytosis at 14 days, but this condition reappeared at day 30 at the time when no inflammatory response was seen in the brain, suggesting that this event may be unrelated to the vector or treatment. Monocytosis was associated with a mild neutrophilia and a lymphopenia in three of the four animals. While remaining within normal ranges, long-term animals demonstrated a 30% increase in platelets from baseline measurements following surgery (days 4 and 14), which returned to baseline by the time of killing (4 weeks). Blood chemistry analyses revealed that with one exception, all test values were within the normal

reference range throughout the study. One animal receiving a mid-dose of vector showed a moderate elevation in alkaline phosphatase.

Generation of anti-HSV antibodies

Adverse events in human gene therapy studies have been associated with inflammatory and immune responses to the vector or transgene products, and thus we determined whether vector inoculation would indeed cause a vector-specific immune response to viral antigens. To ensure that primates had not been previously exposed to herpesvirus antigens, only primates negative for Herpes-B were enrolled in this study. Following intracranial delivery of NUREL-C2, attempts were made to detect the presence of anti-HSV serum antibodies using a 50% HSV plaque reduction assay. All test serum samples were negative even at the lowest dilution (1:1), while the positive control anti-gB antibody showed a 50% decrease in viral titer at a dilution of 1:500. This finding was consistent with the failure of virus to replicate and spread beyond the brain parenchyma where antigen presentation could induce anti-viral immunity, a conclusion supported by the failure to detect viral DNA in other tissues (below).

MRI evaluation

MRI provides information on inflammatory changes or the occurrence of encephalitis in live animal brains that potentially could arise as a result of vector inoculation.²⁶ All primates were subjected to base line imaging prior to surgery. In all cases, MRI showed acute inflammatory changes (abnormal T1 on T1 and abnormal T2 prolongation on FLAIR imaging) at 4 days postinoculation compared to base line. The inflammatory response was limited to the site of vector delivery with mild mass effect but no midline shift. No evidence of inflammation was seen in distant sites in the brain. Long-term changes were studied in two monkeys receiving 1×10^8 and 1×10^9 PFU. In the primate receiving 1×10^8 PFU, the inflammatory reaction seen on day 4 disappeared by day 18 and the brain returned to normal morphology and MR signal pattern. In this animal, no abnormal signal in the brain was detected on day 33. In the primate receiving the highest dose (1×10^9 PFU) (Figure 3), the inflammatory reaction seen on day 4 was still evident at day 17 but the degree of abnormal T1 and T2 prolongation had considerably decreased, the mass effect was minimally decreased and no midline shift was noted. In this animal, MRI from day 32 revealed no abnormal T1 or T2 prolongation in the brain parenchyma on either side, indicating a return to normal morphology and MR signal pattern.

Histopathology

Standard histological examination of brains of study animals affords a more detailed and specific analysis into the reactions to an investigational new drug. External examination of the brain revealed slight discoloration of the cerebral cortex in the injection region in all animals. Petechial hemorrhages were observed at the injection sites. No other gross abnormalities were observed. Immunocytochemical staining for HSV was negative in all animals. Standard hematoxylin and eosin (H&E) staining suggested macrophage infiltration into the needle tract and surrounding meninges (Figure 4). Immunocytochemical staining for the macrophage marker CD68 confirmed the presence of macrophages filling the needle track and infiltrating the meninges of the overlying cortex in all animals (Figure 4). Immunostaining for glial fibrillary acidic protein (GFAP) showed the presence of a diffuse low-grade global gliosis observed as faint brown coloration, more pronounced around the needle track and surface contusion particularly in the long-term animals (Figure 4). There was no evidence of significant lymphocyte infiltration.

Immunohistochemistry

To examine the duration of transgene expression, immunofluorescence for HSV-TK expression was examined in brains of short- and long-term animals. HSV-TK expression was

detected around apparent needle tracts in brains of all animals from the short-term group, but expression was not detected in any long-term animal. HSV-TK immunoreactivity in this higher magnification image was most prominent in the highest dose (1×10^9) and was constrained to the immediate vicinity of injection (Figure 5).

RT-PCR

Since TNF α expression produces an inflammatory response that increases the effectiveness of gamma knife therapy, vector-derived expression should be transient and maximal expression should be coincident with gamma knife delivery. In order to detect specifically vector-derived TNF α expression and not endogenous TNF α expression that is likely induced by surgery, we designed RT-PCR primers specific for the viral polyadenylation signal engineered following the human transgene coding sequence. Expression of vector expressed TNF α was assessed by RT-PCR on RNA isolated from injected and contralateral brain from all animals. Vector-derived TNF α expression was observed in short-term animals in the injected brain region but not in contralateral brain (Figure 6). To evaluate the duration of TNF α expression from NUREL-C2, the same RT-PCR assay was performed on samples purified from long-term animals. As seen for HSV-TK expression by immunofluorescence above, TNF α expression became undetectable in long-term animals, demonstrating the transient nature of transgene expression from this vector in normal brain.

Biodistribution

We determined the gross biodistribution of our HSV-based vector by quantitative PCR (QPCR) for specific HSV sequences on tissues harvested at necropsy. The limit of vector detection of our QPCR assay was determined to be 35 copies of HSV genomes in the presence of 100 ng genomic cell DNA. All QPCR assays were in agreement and could reliably detect HSV viral DNA in the injected region of brain but not in contralateral regions or other body tissues. Figure 7 shows a representative amplification of NUREL-C2 genomes using the U_S6 primers/probe set from the injected brain, but not the contralateral side or liver or testes, of all acute and chronic animals. There were no viral sequences detected above background in any monkey from any other tissue including liver, testicle, lung, heart, spinal cord (cervical, thoracic, and lumbar) kidney, spleen, pancreas, intestine (jejunum, colon, and ileum), and skeletal muscle (leg, back).

Discussion

Human studies with HSV has thus far been limited to the use of replication-competent herpesvirus mutants that restrict virus replication to dividing cells. Tumor cell killing is achieved by lytic virus growth, and thus these mutants have been referred to as oncolytic viruses.^{27,28} The safety and biodistribution of oncolytic HSV viruses have been examined in both rodents and non-human primates following intracranial administration. The oncolytic HSV virus G207, for example, is deleted for γ 34.5 and UL39 (the large subunit of the viral ribonucleotide reductase) and is nonpathogenic^{29,30} following intracerebral inoculation of mice and non-human primates and viral genomes remained localized to the injection site. In addition, oncolytic HSV vectors are unable to reactivate endogenous resident wild-type HSV,^{30,31} suggesting that infection of human brain where HSV may be resident would not lead to virus reactivation and potential encephalitis. Two Phase I clinical trials support this conclusion where application of conditionally replicating HSV vectors do not show evidence of adverse events due to virus growth.^{32,33}

We have carried out preclinical studies in animal models of human brain tumors that suggest highly defective nonreplicating HSV vectors such as NUREL C2 may prove valuable in the treatment of recurrent glioma in patients.^{14,23,34} The toxicology and human studies with

oncolytic vectors provide encouraging evidence that HSV can be safely applied to patients and since defective vectors are incapable of productive infection even in tumor cells, it is unlikely that the defective virus platform will itself pose a safety concern. Nevertheless, vector toxicity may vary with the transgene(s) payload, and thus it is essential to establish that the combination of vector and transgenes can safely be administered to the brains of animals including primates prior to testing in patients.

The goals of this study were to evaluate the possible toxicity associated with intracerebral inoculation of NUREL-C2, a multigene HSV vector under consideration for treatment of patients with recurrent glioma. Our clinical objective is to evaluate the safety of the NUREL-C2 treatment paradigm with and without concurrent gamma knife treatment in patients with recurrent glioma. Since our clinical protocol will require the intracranial injection of a viral vector that may be inherently toxic or show toxicity through the expression of genes intended for tumor killing, we carried out vector toxicity studies in primates as the most relevant model system. The size and organization of the primate brain also allows for inoculation of similar vectors doses to be used in human studies. Moreover, primates afford the opportunity to assess clinical status including behavioral parameters that are more apt to mimic human behavior.

The experiments were carried out in healthy primates using the dose regimen (10^7 – 10^9 PFU) we are proposing for human studies. The animal protocol was designed to determine whether this multigene vector altered the behavioral and clinical status of injected animals in the presence of GCV therapy. In particular, we determined whether (i) the vector remained localized to the injection sites, (ii) induced pathologic changes in brain, or (iii) caused systemic changes that include altered blood chemistry, blood cell populations or stimulated the production of anti-HSV antibodies.

Vector stocks used in these studies were shown to be free of detectable RCV. We validated our RCV assay by introducing 3 PFU RCV into a vector sample containing 10^9 vector particles. In each case, RCV was detected in these spiked samples indicating our level of sensitivity is less than 3 PFU per test dose. When representative samples of the vector preparation were tested, no RCV was detected on noncomplementing Vero cells. The likelihood that RCV will arise during virus production is very low since multiple essential virus genes (ICP27 and ICP4) must be rescued for production of active virus raising our confidence that our vector stocks were free of RCV. The complementing cell lines were carefully engineered to minimize homologous sequences with the vector and thus rescue necessitates several illegitimate recombination events.

Biodistribution

The Taqman QPCR assays used to evaluate vector distribution were capable of detecting less than 10 copies per reaction using either plasmids known to contain the target sequences or pure viral DNA as the template. Assays to detect viral sequences in the presence of cellular genomic DNA (extracted from Vero cells or *M. mulatta* tissue), reduced the sensitivity to 35 copies per reaction due to increased background. We utilized three sets of primer/probes and separate QPCR instruments with similar results. The results of these studies showed the presence of viral DNA limited to the injected sites of the brain. At 4 days postinoculation, approximately 1–3% of the total virus dose was detected at the injection site that declined approximately 10-fold by 4 weeks postinjection. The method of tissue extraction and sampling for PCR analysis in the brain was limited to one injection site of 10, thus these are only approximations of genome copy number per inoculated brain. Studies to detect virus in uninjected sites were negative and included important tissues such as contralateral brain regions, cervical spinal cord, liver, and testes. These findings confirm that virus spread either does not occur or occurs at very low levels by this route of administration and is in agreement with findings reported for oncolytic HSV vectors.^{29,30,34}

Brain pathology

In general, the pattern of brain changes in injected animals consisted of an inflammatory response, the appearance of inflammatory cells such as macrophages and a diffuse low-grade gliosis. Most changes resolved over the 4-week time course of the experiments and declined in a manner that corresponded to the kinetics of vector transgene expression, which also became undetectable at 4 weeks. A transient inflammatory response was detected by MRI with corresponding and declining numbers of infiltrating CD68-positive macrophages during the 4-week study period. The apparent inflammation detected by MRI appeared less severe at 2 weeks postinjection, resolving by 4 weeks and occurred in a distribution similar to the injection pattern.

As TNF α is a proinflammatory cytokine, the localized response seen in brain was expected. Previous studies by us and others have shown that local TNF α production provides multiple benefits to cancer gene therapy and include the recruitment of nonspecific antitumor cellular responses and increased the effectiveness of radiation therapy and GKR.²⁰⁻²² The expression of TNF α was vigorous during the initial phase of the study and rapidly declined to undetectable levels at 4 weeks postinoculation as documented by RT-PCR. We did not determine whether increased levels of TNF were present in the blood; however, the injected animals showed no behavioral changes or weight loss.

Histopathology studies of the injected sites did not reveal any gross loss of neurons at the injection sites. Although the vector expresses the viral tk and ICP0 gene products and the rat CX43 and human TNF α gene products, these transgene products did not lead to overt destruction of normal brain tissue. While ICP0 can cause cell cycle arrest in dividing cells, neurons are apparently unaffected and indeed this protein has been shown to be degraded in neurons.⁴ The animals were also given GCV that is activated by viral TK, but again the use of this drug did not induce cytotoxic changes in normal brain. Together, these data support the safety of this multigene vector for intracranial applications.

Systemic changes

Blood cell analysis revealed a mild monocytosis in several animals. However, these same animals had elevated monocytes at baseline measurements, suggesting that this is not related to vector delivery but most likely was indicative of a stress-related response due to procedures and handling. However, the animals did show an ~30% increase from baseline in platelet levels after surgery that returned to baseline levels after 4 weeks. This increase was independent of vector titer, suggesting that the effect was related to animal handling or surgery. In preclinical toxicology studies in rodents using an adenoviral vector that expresses TNF α (TNFerade), a decrease in hemoglobin (~19%) and increases in platelets (~100%) and white blood cells (300%) was documented.²¹ In the TNFerade study, however, high doses of vector were repeatedly injected subcutaneously and lead to ulceration and necrosis at the injection site, while our study involved a single intracranial injection time point. Unlike the TNFerade vector, our vector did not induce any significant changes in animal weight or in the WBC differentials.

It might be expected that exposure to virus outside the brain would induce the production of anti-viral antibodies and seroconversion. We therefore tested for the presence of anti-HSV antibodies using a virus neutralization assay. The results showed that even undiluted animal serum did not contain antibody capable of neutralizing the HSV-1 KOS strain used as the backbone for our vector.

These studies demonstrate that NUREL-C2 can be produced and purified without the generation of RCV contamination of vector preparations. In the treatment of cancer, short-term, high-level expression of multiple transgenes results in rapid tumor killing and the

attraction of a cellular response to the tumor site may be desirable for destruction of remaining tumor cells. High-level expression maximizes the therapeutic effects of concomitant GCV and GKR and minimizes the vector dosing required to achieve this effect. Transient transgene expression from a nonintegrating vector provides a safety factor by reducing the potential of unwanted distant or long-term expression effects as well mitigating the possibility of insertional mutagenesis or oncogene activation effects. Immunohistochemistry for nonendogenous gene products (such as HSV-TK) and several animal time points affords us the opportunity to document the nature of transgene expression in this setting without visualizing endogenous cell gene products (ie any primate TNF α response). We found no evidence of spread of vector genomes from the site of injection or generation of anti-HSV antibodies. Transgene expression is transient as was the inflammatory response visualized by MRI. In summary, NUREL-C2 can be safely administered to primate brain at doses up to 1×10^9 , the same maximum dose that is planned for use in human clinical trials.

Materials and methods

Construction and production of NUREL-C2

The construction and effectiveness of NUREL-C2 has been described previously.¹⁴ Briefly, the following modifications were made in the background of the laboratory strain KOS; the essential IE gene ICP4 was deleted, originally designated d120;³⁵ the essential IE gene ICP27 was deleted³⁶ and an HCMV-EGFP cassette inserted at the ICP27 locus;²⁴ the VP16-responsive TATGARAT elements in the promoters of ICP22 and ICP47 were removed converting their expression profile from IE to early;²⁴ the natural TK (U_L23) promoter was replaced with the ICP4 IE promoter to provide high-level expression in noncomplementing cells;⁶ a dual expression cassette consisting of the ICP0 IE promoter driving rat CX43 cDNA and the HCMV IE promoter driving expression of the human TNF α cDNA were inserted into the UL41 locus (Figure 1).¹⁴

The vector was produced using good laboratory practices in roller bottles on complementing E11 cells²⁴ and purified on a continuous nycodenze gradient. Vector stock aliquots were titered on complementing E11 cells and stored at -80°C . All tissue culture medium and serum was obtained from Invitrogen (Carlsbad, CA, USA)

Replication-competent HSV detection assay

Stocks of vectors were assayed for potential replication-competent recombinant virus on noncomplementing Vero cells. A measure of 10 ml containing 1×10^8 Vero cells were infected in suspension with: (1) 3 PFU KOS, (2) 1×10^8 PFU NUREL-C2, (3) 1×10^9 PFU NUREL-C2, (4) 3 PFU KOS plus 1×10^8 PFU NUREL-C2, or (5) 3 PFU KOS plus 1×10^8 PFU NUREL-C2 and seeded into roller bottles in a total of 100 ml DMEM with 10% fetal calf serum. At 3 days after infection, the cells and supernatant from each roller bottle were harvested with sterile disposable cell scrapers (Fischer Scientific, Pittsburgh, PA, USA), the cells pelleted by centrifugation at 1000 g for 10 min. The supernatant was reserved and the cell pellet subjected to three freeze/thaw cycles, centrifuged, and added back to the supernatant. The resulting cell lysate was clarified by centrifugation (1000 g for 5 min) and the virus pelleted by centrifugation (20 000 g for 30 min) and resuspended in 1 ml of media. A total of 1×10^7 Vero cells were infected with the resulting viral preparation, plated in T150 tissue culture flasks and assayed for PFU or complete CPE 3 days later by crystal violet staining (1% in 50% methanol).

Animals

Five male Indian origin rhesus macaques (*M. mulatta*), seronegative for herpes B virus (cercopithecine herpesvirus 1) and ranging in age from 5 to 13 years old, were used for the

study. Activity level, stool consistency, appetite, and general condition were observed twice daily. Physical examinations were performed prior to sample collection or surgical manipulations and consisted of body temperature and weight measurements, palpation and size grading of lymph nodes and spleen, abdominal palpation, and assessment of general condition. The five macaques were separated into an acute group ($n = 3$; killed within 4–6 days following NUREL-C2 treatment) and a chronic group ($n = 2$; killed within 35 days following NUREL-C2 treatment).

All five monkeys had MRI imaging performed at baseline and at 4 days following NUREL-C2 delivery. The chronic group had additional imaging performed at approximately 2 and 4 weeks following NUREL-C2 injection. Blood, nasal swabs, urine, and CSF samples were collected prior to all imaging studies. These analyses were carried out by Infectious Disease Diagnostic Laboratories at the University of Pittsburgh Medical Center (UPMC). Complete blood cell (CBC) measurements included HgB, Hct, RBC, MCV, MCH, MCHC, RDW, WBC, MPV, platelets, differential percent neutrophils, lymphocytes, monocytes, eosinophils, and basophils. Blood chemistry panel measurements included albumin, ALT (alanine aminotransferase), AST (alkaline phosphatase), calcium, creatinine, gGTP (gamma-glutamyl transferase), glucose, electrolytes: sodium (Na), potassium (K), chloride (Cl), carbon dioxide, (CO_2), phosphorus, total bilirubin, total protein, and urea nitrogen. All five animals had craniotomies performed prior to injection of the NUREL-C2 vector and GCV-filled Alzet osmotic pumps (Alzet; Cupertino, CA, USA) were implanted subcutaneously (below).

This study was approved prior to initiation by the University of Pittsburgh Institutional Biosafety Committee (IBC) and Institutional Animal Care and Use Committee (IACUC).

Surgery

Vector Inoculation—An animal sedated with ketamine (10 mg/kg) intramuscularly (i.m.) and medetomidine IM (25 $\mu\text{g}/\text{kg}$) and anesthetized with isoflurane (2%) was placed prone with a chin support and the head was cleaned and prepared using scrub betadine and alcohol. Head, neck and body were covered using disposable sterile drapes. A linear parasagittal incision was made in the right frontal scalp region and skin was retracted using self-retaining retractors. The underlying muscle was split and retracted and the pericranium was incised and stripped off the bone. A 2 cm \times 2 cm free bone flap craniotomy was performed using a pneumatic drill and cutters. The dura mater was opened in a cruciate manner. Upon opening the dura, normal frontal cortex was noted. Each monkey received 10 aliquots of 10 μl each of the NUREL-C2 vector spaced equidistantly around the perimeter of the craniotomy site to mimic injections into the boundaries of a tumor mass. Each aliquot of vector was infused slowly over 3 min placed at a depth of approximately 5 mm into the exposed cortex. Each monkey received a total of 100 μl containing 1×10^7 ($n = 1$), 1×10^8 ($n = 2$), or 1×10^9 ($n = 2$) PFU purified NUREL-C2 vector. After vector delivery, the dura was closed with sutures and covered by surgical seal. The bone flap was replaced and the scalp was closed in layers.

Osmotic pump implantation—Osmotic pumps (Alza Corp, Palo Alto, CA, USA) were implanted between the shoulder blades within a subcutaneous pocket formed by blunt dissection. An Alzet pump model 2LM1 (10 $\mu\text{l}/\text{h}/7\text{days}$) was used for acute animals and two model 2LM2 (5 $\mu\text{l}/\text{h}/14\text{days}$) pumps for chronic animals. Pumps were filled with GCV (Cytovene, Roche, Nutley, NJ, USA) at a concentration (<500 mg/ml) to deliver a dose of 10 mg/kg/day. In chronic animals, the osmotic pumps were replaced 2 weeks after the craniotomy following the 2 week MRI.

Magnetic resonance imaging—All monkeys were sedated with ketamine (10 mg/kg) i.m. and medetomidine IM (25 $\mu\text{g}/\text{kg}$) prior to imaging. MRI was performed at the UPMC MR

Research Center using 1.5 T sigma MR unit (General Electric). Baseline MRI was performed on all five monkeys 2 days prior to vector injection. Both T1- and T2-weighted MR sequences were performed. T1 waiting was performed using FSE (fast spin echo) sequence in central and axial planes. Axial FSEIR (fast spin echo inversion recovery) sequence was performed to emphasize T2 information without exogenous contrast administration. To study and document the short-term changes, all five monkeys underwent MRI using the same sequences 4 days after intracranial injection of NUREL-C2 into the right frontal cortex. The two chronic monkeys, who received 10^8 and 10^9 PFU vector in 100 μ l, had additional MRI 2 and 4 weeks after vector delivery using the same MR sequences.

Sample collection—Animals were chemically restrained with ketamine i.m. (10 mg/kg) and blood was drawn from the femoral vein. CSF was collected via cisternal puncture and cystocentesis was performed to collect urine samples. All animals were chemically restrained with ketamine i.m. (10 mg/kg) prior to euthanasia with intravenous (i.v.) Beuthanasia-D (65 mg/kg). Organ samples including brain (injected and contralateral), spinal cord (cervical, thoracic and lumbar), heart, liver, lung, kidney, intestine, testes, and muscle were individually vial for (1) DNA extraction for PCR analysis by snap freezing and (2) backup immunohistochemical processing by embedding in optimal cutting temperature prior to freezing in liquid nitrogen. Tissue specimens were collected using disposable scalpels and separate sets of sterilized instruments.

Testing for anti-HSV antibodies—In order to detect an anti-HSV immune response, HSV neutralization assays were performed on serum samples collected from animals prior to virus inoculation and at all subsequent time points to detect anti-HSV antibodies possibly induced by intracranial virus injection. Dilutions (1:1–1:5000) of each serum sample and controls (no serum, anti HSV pAb³⁷) were incubated with 200 PFU of HSV (strain KOS) in 500 μ l media (DMEM/10%FBS) for 90 min at 37°C. The resulting serum–HSV mixture was added to 7.5×10^5 freshly trypsinized Vero cells in 500 μ l and incubated on a rocking platform for an additional 90 min at 37°C. The infections were plated in six-well tissue culture dishes and washed with glycine 2 h postplating to inactivate extracellular virus. The infected cells were overlaid with 1% methylcellulose/DMEM/10% FBS and incubated for 2 days at 37°C. Plaques were counted after staining with Crystal Violet.

Histopathology and immunohistochemistry—Brains were fixed for 1 week in 10% formalin. After fixation, the cerebrum was sectioned in the coronal plane and the cerebellum and brainstem in the horizontal plane. Ipsilateral and contralateral sections were embedded in paraffin and stained with H&E. Immunocytochemical staining was performed with the following antibodies: mouse anti-human GFAP (Dako Corp, Carpinteria, CA, USA; #M0761 at 1:1000), mouse anti-human macrophage CD68 (Dako Corp; #M0814 at 1:100), rabbit anti-HSV (Dako Corp; #B0114 at 1:500), and rabbit anti-HSV thymidine kinase (1:500).³⁸ Secondary antibodies were goat anti-rabbit or goat anti-mouse (Dako Corp) visualized with AEC (Aminoethyl carbazole) or Cy3-conjugated rabbit anti-mouse antibody (1:500) (Sigma).

RT-PCR

RNA from injected and contralateral brain was extracted using RNEasy (Qiagen, Valencia, CA, USA) and subjected to RT-PCR analysis using primers specific for vector derived TNF α . Total RNA 50 ng was used with Superscript One-Step RT-PCR for Long Templates (Invitrogen) in a 50 μ l reaction volume using a Robocycler (Stratagene, La Jolla, CA, USA) PCR instrument. RT-PCR conditions were 30 min, 50°C, 96°C, 2 min, and 35 cycles of 95°C, 20 s, 62°C, 20 s, and 68°C, 20 s. Primers, used at 0.25 μ M, included TNFU1 CCGAGTGACAAGCCTGTAGCC and TNFL1 CCTTGAAGAGGACCTGGGAGT. RT-

PCR products were analyzed by 2.5% agarose-gel electrophoresis. Ethidium bromidestained gel images were captured with a Kodak DC120 gel documentation system.

Quantitative PCR

Samples were processed using a DNeasy Tissue kit as described (Qiagen). Initially, viral preparations were quantified for two viral sequences present in the replication-defective vectors; U_S6 (glycoprotein D) and U_L53 in duplicate. Assays were conducted in 50 µl containing 2 µl DNA sample, 200 nM of each primer, 200 nM Probe, and 25 µl TaqMan 2 × Universal Master Mix (PE Applied Biosystem, Foster City, CA, USA). Primer sequences for U_S6 (gD) (sense: CCC CGC TGG AAC TAC TAT GAC A; and antisense: GCA TCA GGA ACC CCA GGT T), and U_L53 (ICP27) (sense: GGG CCT GAT CGA AAT CCT AGA; and antisense: GCC GTC AAC TCG CAG ACA) were designed using the ABI Prism Primer Express software (PE Applied Biosystem). TaqMan probes for detection of U_S6 (TTC AGC GCC GTC AGC GAG GA) and U_L53 (CGC ACC GCC AGG AGT GTT CGA G) were labeled with fluorescent reporter dye 6-FAM at the 5'-end and TAMRA quencher at the 3'-end (PE Applied Biosystem). PCR reactions were setup in a MicroAmp Optical 96-well Reaction Plate (PE Applied Biosystem). Amplification conditions were 2 min at 50°C and 10 min at 95°C for the first cycle, followed by 50 cycles of 95°C for 15 s and 60°C for 1 min. Standards curves for viral sequences, U_S6 and U_L53, were generated using 10-fold serial dilutions of plasmids known to contain the target sequences, pgDSac and pPxe, respectively. Accuracy and correlation between plasmid standard curves and viral genomes was confirmed by including a series of dilutions of viral stock whose particle number was determined by negative staining electron microscopy. Known negative samples were spiked with dilutions of plasmid standards to determine limits of detection. The emission data were collected in real-time from an ABI PRIME 7700 Sequence Detector and transferred to a Macintosh 7100 for analysis using Sequence Detector V1.6 (PE Applied Biosystem).

To further confirm these biodistribution studies, an independent assay was utilized using an Applied Biosystems GeneAmp® 5700 Sequence Detection System and Real-time TaqMan® PCR (Applied Biosystems, Foster City, CA, USA). Real-time PCR reactions were setup as follows: 5 µl sample, 0.225 µl each of 200 µM forward and reverse primers, 0.125 µl of 100 µM TaqMan probe, 25 µl of 2 × TaqMan Universal PCR Master Mix, and 19.425 µl nucleotide-free water. Dilutions of NUREL-C2 viral DNA was used as a positive control. In all, 50 cycles of amplification were performed: 95°C, 15 s melting, 60°C, 1 min annealing/extension. ABI PRISM Primer Express software was used to design a primer/probe set for the HSV U_L27 gene (forward primer 5'-gcagtactacctggccaatgg-3'; reverse primer 5'-GCGAGCGTGTGCTGAGA-'; TaqMan probe 5'-FAM-TTTCTGATCGCGTACCAGCCC-TAMRA-3' (Synthegen, Houston, TX, USA).

Acknowledgements

We thank Mellanie Osborn and Anna Jones for animal handling and technical assistance during surgery and MRI evaluations. This research is supported by NGVL 1U42RR1657901 and NIH 1P01NS40923-01A1.

References

1. Hochberg F, Pruitt A. Assumptions in the radiotherapy of glioblastoma. *Neurology* 1980;30:907–911. [PubMed: 6252514]
2. Prados M, Levin V. Biology and treatment of malignant glioma. *Semin Oncol* 2000;27:1–10. [PubMed: 10866344]
3. Wallner K, et al. Patterns of failure following treatment for glioblastoma multiforme and anaplastic astrocytoma. *Int J Radiat Oncol Biol Phys* 1980;16:1405–1409. [PubMed: 2542195]
4. Chen X, et al. Herpes simplex virus type 1 ICP0 protein does not accumulate in the nucleus of primary neurons in culture. *J Virol* 2000;74:10132–10141. [PubMed: 11024142]

5. Samaniego L, Neiderhiser L, DeLuca N. Persistence and expression of the herpes simplex virus genome in the absence of immediate-early proteins. *J Virol* 1998;72:3307–3320. [PubMed: 9525658]
6. Krisky D, et al. Development of herpes simplex virus replication-defective multigene vectors for combination gene therapy applications. *Gene Therapy* 1998;5:1517–1530. [PubMed: 9930305]
7. Germano I, Fable J, Gulteki S, Silvers A. Adenovirus/herpes simplex-thymidine kinase/ganciclovir complex: preliminary results of a phase I trial in patients with recurrent malignant gliomas. *J Neuro-Oncol* 2003;65:279–289.
8. Smitt P, et al. Treatment of relapsed malignant glioma with an adenoviral vector containing the herpes simplex thymidine kinase gene followed by ganciclovir. *Mol Ther* 2003;7:851–858. [PubMed: 12788659]
9. Trask T, et al. Phase I study of adenoviral delivery of the HSV-tk gene and ganciclovir administration in patients with current malignant brain tumors. *Mol Ther* 2000;1:195–203. [PubMed: 10933931]
10. Dilber MS, et al. Gap junctions promote the bystander effect of herpes simplex virus thymidine kinase *in vivo*. *Cancer Res* 1997;57:1523–1528. [PubMed: 9108455]
11. Mesnil M, et al. Bystander killing of cancer cells by herpes simplex virus thymidine kinase gene is mediated by connexins. *Proc Natl Acad Sci USA* 1996;93:1831–1835. [PubMed: 8700844]
12. Wu JK, et al. Bystander tumoricidal effect in the treatment of experimental brain tumors. *Neurosurgery* 1994;35:1094–1102. [PubMed: 7885554]
13. Marconi P, et al. Connexin43-enhanced suicide gene therapy using herpesviral vectors. *Mol Ther* 2000;1:71–81. [PubMed: 10933914]
14. Niranjana A, et al. Treatment of rat gliosarcoma brain tumors by HSV-based multigene therapy combined with radiosurgery. *Mol Ther* 2003;8:530–542. [PubMed: 14529825]
15. Kondziolka D, et al. Survival benefit of stereotactic radiosurgery for patients with malignant glial neoplasms. *Neurosurgery* 1997;41:776–785. [PubMed: 9316038]
16. Loeffler J, et al. Radiosurgery as part of the initial management of patients with malignant gliomas. *J Clin Oncol* 1992;10:1379–1385. [PubMed: 1325539]
17. Baher A, et al. A model using radiation and plasmid-mediated tumor necrosis factor-alpha gene therapy for treatment of glioblastomas. *Anticancer Res* 1999;19:2917–2924. [PubMed: 10652573]
18. Gridley D, et al. TNF-alpha gene and proton radiotherapy in an orthotopic brain tumor model. *Int J Oncol* 2002;21:251–259. [PubMed: 12118318]
19. Weichselbaum R, et al. Radiation-induced tumour necrosis factor- α expression: clinical application of transcriptional and physical targeting of gene therapy. *Lancet Oncol* 2002;3:665–671. [PubMed: 12424068]
20. Chung T, et al. Tumor necrosis factor-alpha-based gene therapy enhances radiation cytotoxicity in human prostate cancer. *Cancer Gene Therapy* 1998;5:344–349. [PubMed: 9917088]
21. Rasmussen H, et al. TNFerade biologic: Preclinical toxicology of a novel adenovector with a radiation-inducible promoter, carrying the human tumor necrosis factor alpha gene. *Cancer Gene Ther* 2002;9:951–957. [PubMed: 12386834]
22. Staba M, et al. Adenoviral TNF-alpha gene therapy and radiation damage tumor vasculature in a human malignant glioma xenograft. *Gene Therapy* 1998;5:293–300. [PubMed: 9614548]
23. Niranjana A, et al. Effective treatment of experimental glioblastoma by HSV vector-mediated TNF- α and HSV-tk gene transfer in combination with radiosurgery and ganciclovir administration. *Mol Ther* 2000;2:114–120. [PubMed: 10947938]
24. Samaniego L, Webb A, DeLuca N. Functional interaction between herpes simplex virus immediate-early proteins during infection: gene expression as a consequence of ICP27 and different domains of ICP4. *J Virol* 1995;69:5705–5715. [PubMed: 7637016]
25. Wolfe D, et al. Herpesvirus-mediated systemic delivery of nerve growth factor. *Mol Ther* 2001;3:61–69. [PubMed: 11162312]
26. Koelfen W, et al. MRI of encephalitis in children: comparison of CT and MRI in the acute stage with long-term follow-up. *Neuroradiology* 1996;38:73–79. [PubMed: 8773284]
27. Shah A, Benos D, Gillespie G, Markert J. Oncolytic viruses: clinical applications as vectors for the treatment of malignant gliomas. *J Neuro-Oncol* 2003;65:203–226.

28. Varghese S, Rabkin S. Oncolytic herpes simplex virus vectors for cancer virotherapy. *Cancer Gene Ther* 2002;9:967–978. [PubMed: 12522436]
29. Hunter W, et al. Attenuated, replication-competent herpes simplex virus type 1 mutant G207: safety evaluation of intracerebral injection in nonhuman primates. *J Virol* 1999;73:6319–6326. [PubMed: 10400723]
30. Sundaresan P, Hunter W, Martuza R, Rabkin S. Attenuated, replication-competent herpes simplex virus type 1 mutant G207: Safety evaluation in mice. *J Virol* 2000;74:3832–3841. [PubMed: 10729157]
31. Loudon P, et al. Preclinical safety testing of DISC-hGMCSF to support phase I clinical trials in cancer patients. *J Gene Med* 2001;3:458–467. [PubMed: 11601759]
32. MacKie R, Stewart B, Brown S. Intralesional injection of herpes simplex virus 1716 in metastatic melanoma. *Lancet* 2001;357:525–526. [PubMed: 11229673]
33. Markert J, et al. Conditionally replicating herpes simplex virus mutant, G207 for the treatment of malignant glioma: results of a phase I trial. *Gene Therapy* 2000;7:867–874. [PubMed: 10845725]
34. Deisboeck T, et al. Development of a novel non-human primate model for preclinical gene vector safety studies. Determining the effects of intracerebral HSV-1 inoculation in the common marmoset: a comparative study. *Gene Therapy* 2003;10:1225–1233. [PubMed: 12858187]
35. DeLuca N, McCarthy A, Schaffer P. Isolation and characterization of deletion mutants of Herpes simplex virus type 1 in the gene encoding immediate-early regulatory protein ICP4. *J Virol* 1985;56:558–570. [PubMed: 2997476]
36. McCarthy A, McMahan L, Schaffer P. Herpes simplex virus type 1 ICP27 deletion mutants exhibit altered patterns of transcription and are DNA deficient. *J Virol* 1989;63:18–27. [PubMed: 2535723]
37. Highlander S, et al. Monoclonal antibodies define a domain on herpes simplex virus glycoprotein B involved in virus penetration. *J Virol* 1988;62:1881–1888. [PubMed: 2452895]
38. Summers W, Wagner M, Summers W. Possible peptide chain termination mutants in thymidine kinase gene of a mammalian virus, herpes simplex virus. *Proc Natl Acad Sci, USA* 1975;72:4081–4084. [PubMed: 172894]



Figure 1. Diagram of wild-type HSV (KOS) and the replication-defective vector (NUREL-C2) used in this study. Open boxes represent terminal (T) or internal (I) repeated (R) elements flanking the unique long (U_L) and unique short (U_S) regions. Deletions and insertions and their relevant loci are indicated to the right of the figure.

**Figure 2.**

Flowchart of procedures performed. All animals were negative for Herpes-B on two independent tests prior to being enrolled in this study. Vector was produced and purified as described in Materials and methods and vector lots tested negative for RCV prior to use. At 2 days before surgery, the animals underwent a full examination consisting of a routine physical exam, MRI, CBC, and blood chemistry. Craniotomy, vector injection, and GCV pump implantation was performed as described in Materials and methods on day 0. At 4 days postinjection all animals received a second full standard examination. The acute panel of animals (4 days postinjection) was killed and necropsy processed for histopathology, immunohistochemistry, DNA, and RNA isolation. Both 2 and 4 weeks postinjection full examinations were again performed. Following the 4-week exam, the chronic animals were killed and necropsy processed as for acute animals.

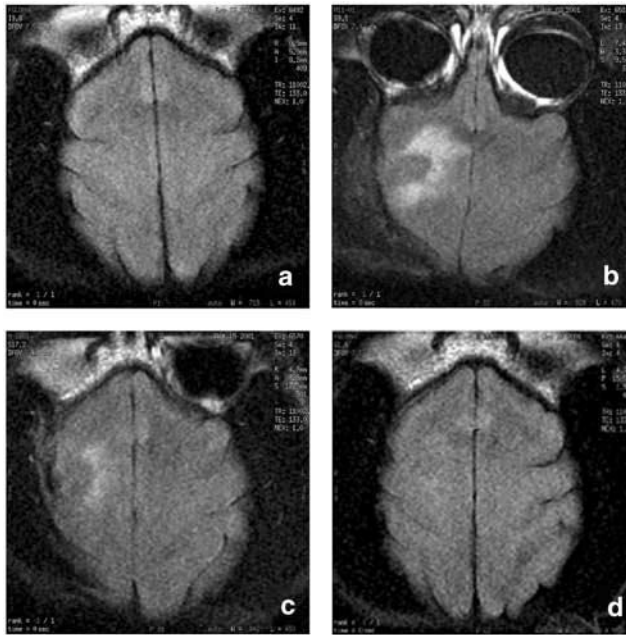


Figure 3.

MRI of the high-dose long-term animal. MRI scans were performed to ascertain the course of (a) Baseline MRI displayed normal brain structure and appearance. (b) At 4 days postinjection of 1×10^9 PFU NUREL-C2, MRI revealed an apparent inflammatory response in the same circular pattern as vector injection. The inflammatory response was reduced after 2-weeks (c) and resolved by 4 weeks (d) postinjection when the brain returned to normal appearance.

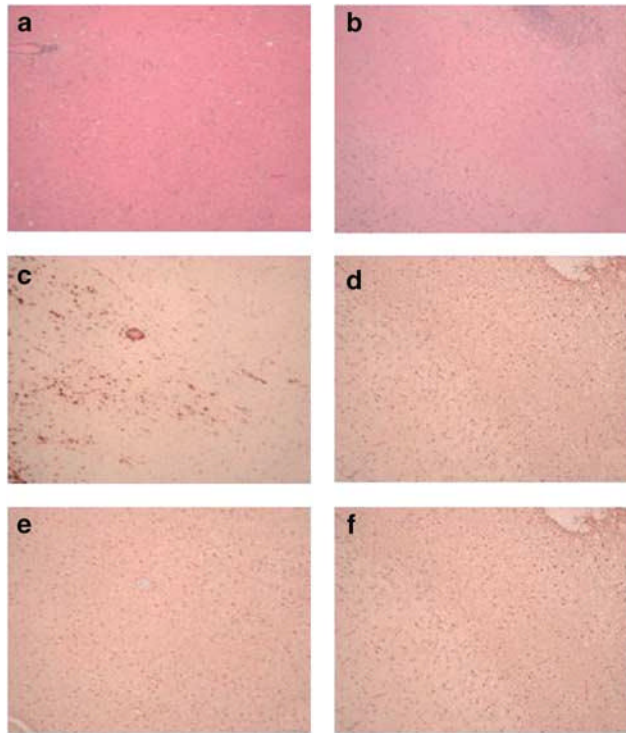


Figure 4. Representative histopathologic evaluation of brain sections from animals injected intracranially with 1×10^9 PFU NUREL-C2. Staining with H&E of the acute (a) or chronic (b) animal brain revealed the presence of the needle tract with cell infiltrates but without gross disruption of the brain architecture. Staining for the macrophage marker CD68 revealed the presence of macrophages in both the acute (c) and chronic (d) animals. The presence of a diffuse low-grade gliosis is observed in both acute (e) and chronic (f) animals using anti-GFAP antibodies.

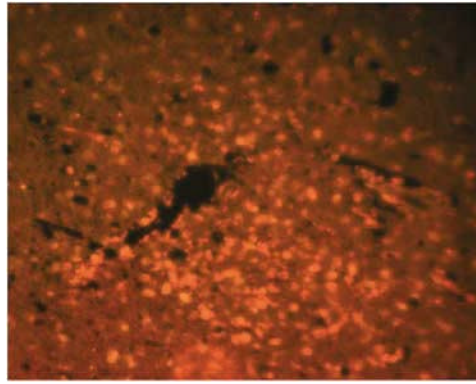


Figure 5. Immunofluorescence staining of HSV-TK in the acute animal treated with 1×10^9 PFU of NUREL-C2. TK immunoreactivity is seen surrounding and extending from the needle track. In NUREL-C2, the TK gene is expressed from the IE ICP4 gene promoter affording high-level expression in the absence of viral replication.

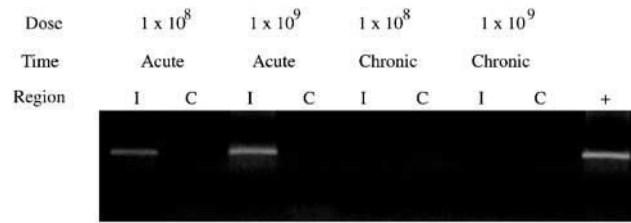


Figure 6.

RT-PCR for viral expressed TNF α . The presence of viral-derived TNF α mRNA was documented by RT-PCR using primers specific for vector delivered TNF α . TNF α expression is seen in the injected (I) but not contralateral (C) brain regions in acute animals at 1×10^8 and 1×10^9 PFU doses. No expression is observed in brain samples harvested from chronic animals injected with 1×10^8 and 1×10^9 PFU NUREL-C2. Positive control (+) was RNA isolated from NUREL-C2-infected Vero cells.

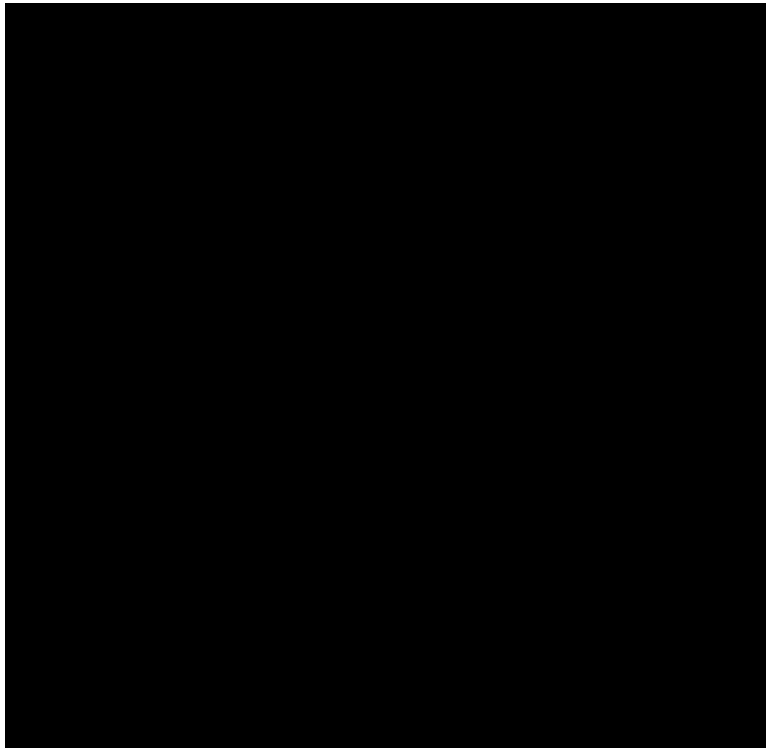


Figure 7. Biodistribution of NUREL-C2 after intracranial delivery. QPCR using primers specific for the HSV vector (gD) were to used to document the presence of NUREL-C2 genomic DNA in samples taken from all animals. The level of sensitivity of this assay is 35 copies of NUREL-C2 DNA per reaction and is indicated by a star. The standard curve was generated using plasmid (pgDSac) that contains the target sequence and are indicated (x). Samples of brain from injected regions were shown to contain NUREL-C2 vector genomes in both chronic and acute groups with the highest levels seen with the acute animal that received the highest vector dose (1×10^9 PFU). Contralateral brain and all other tissues (representative data presented) were negative for the presence of vector genomes.

Table 1

RCV detection assay results

PFU NUREL-C2	PFU KOS	Replication in Vero cells
0	3	+
0	3	+
0	10	+
1×10^8	3	+
1×10^8	3	+
1×10^8	3	+
1×10^8	0	-
1×10^8	0	-
1×10^8	0	-
1×10^9	3	+
1×10^9	3	+
1×10^9	0	-
1×10^9	0	-

Table 2

Animal demographics

Animal #	Dose (total PFU)	Duration (days)	Age (years)	Weight (kg)
M8399	1×10^7	4	10.6	9.3
M1801	1×10^8	5	12.3	13.1
M9001	1×10^9	5	3.8	5.5
M0901	1×10^8	35	6.7	7.5
M1101	1×10^9	34	6.7	7.0